drainage. Proc., HRB, Vol. 31, 1952, pp. 643-666.
15. R. C. Bates and W. R. Wayment. Laboratory Study of Factors Influencing Waterflow in Mine Backfill-Classified Mill Tailings. Bureau of Mines, U.S. Department of the Interior, R.I. 7034, Oct. 1967, pp. 1-27.
16. H. K. Mittal and N. R. Morgenstern. Parameters for the Design of Tailings Dams. Canadian Geotechnical Journal, Vol. 12, No. 2, May 1975, pp. 235-261.

*Publication of this paper sponsored by Committee on Subsurface Drainage.*

**Mr. Elnaggar was on the faculty of the University of Pittsburgh when this research was done.*

# Soil Stresses and Displacements in a Concrete Pipe Trench Installation

Ross B. Corotis and Raymond J. Krizek, Technological Institute, Northwestern University
Thomas H. Wenzel,* Department of Civil Engineering, Marquette University

**The field performance of a full-scale reinforced concrete pipe in a trench installation is described. Total normal stresses were measured by specially designed stress cells placed in the soil and at the soil-pipe interface. Relative displacements between the pipe wall and various discrete points in the soil immediately adjacent to the pipe were determined by means of settlement plates with stems extending through sleeves into the pipe. Stresses and relative displacements, as well as horizontal and vertical diameter changes, were monitored periodically as the height of cover above the pipe increased. In general, the experimental measurements are mutually consistent and compatible with previous experience and judgment; however, there are some differences between the experimental data and the results calculated from a plane strain, finite element model with appropriate soil parameters.**

Described here is the field performance of a full-scale reinforced concrete pipe buried in a trench installation. Instrumentation was provided to measure the normal stresses at the soil-pipe interface and in the adjacent soil, the displacements in the soil above and below the pipe, and deformations of the pipe. Experimental measurements are shown to be mutually compatible and in qualitative agreement with intuitive expectations based on engineering judgment. Typical results at discrete points in the soil-pipe system are compared with values calculated by use of a plane strain, finite element model and soil parameters determined, insofar as possible, from uniaxial strain tests and triaxial compression tests on the actual disturbed and undisturbed soils from the field installation.

## FIELD EXPERIMENT

The test site, which is shown in Figure 1, is located in East Liberty, Ohio, about 64 km (40 miles) northwest of Columbus, on the grounds of the Transportation Research Center of Ohio. A 1.5-m (60-in) inside diameter, 2300 D, B-wall concrete pipe (manufactured by the wet cast method) was installed in a trench with a cover of 7.6 m (25 ft). The required strength of the pipe was determined by means of the Marston-Spangler theory, and the pipe was installed in accordance with the specifications of the Ohio Department of Transportation. The pipe size selected is the result of a compromise between the smallest pipe that allowed reasonable access of personnel and instruments and the largest pipe that could be used with the available cover height, which was dictated by topography and economics. As shown in Figure 2, the installation consists of five 2.4-m (8-ft) lengths of instrumented pipe (the middle one of which is most heavily instrumented), several buffer sections at either end, and a vertical access shaft.

Prior to the manufacture of these pipe sections, an instrumented pipe was tested to ultimate load in a three-edge bearing test to ascertain (a) that the inclusion of internal instrumentation (with the associated holes and inserts) in the pipe cross section would not measurably reduce the strength of the section, (b) that the techniques for applying the instrumentation within the walls of the pipe were adequate to protect the instrumentation during casting, and (c) that measured results (when interpreted within the context of a theoretical model of the pipe only) realistically represent the actual values. Since the results of this test were favorable, the pipe sections for the field installation were manufactured in a similar manner.

The installation of the test pipe was undertaken in June 1971 and was completed within a period of 9 d. As indicated in the boring log shown in Figuro 3, two distinct soils were encountered during excavation. To a depth of approximately 3.7 m (12 ft) there was a coarse to very fine sand with stone fragments and some silt, and from 3.7 m (12 ft) to about 9.1 m (30 ft) there was a dark gray clayey silt; at a point about 9.1 to 10.7 m (30 to 35 ft) below the surface a very granular layer and considerable water were encountered. The soil increased in silt content with depth from 10.7 to 12.8 m (35 to 42 ft), at which point the boring was terminated. The pipe was bedded at a level about 9.4 m (31 ft) below the surface. As a consequence of the unstable nature of the top 4.5 to 6.0 m (15 to 20 ft), the trench was excavated with somewhat unsymmetrical, sloped sides with an approximate 1:1 ratio on one side and about 0.7:1 on the other as shown in Figure 2b; the width of the trench varied from about 3.0 to 3.7 m (10 to 12 ft); the greater width was near the vertical access shaft. Some photographs of the test installation are shown in Figure 4.

Although the laying of the pipe was done basically in accordance with practices recommended by the state of Ohio, a few points are worthy of note. First, the 15 cm (6 in) of compacted granular material at the bottom of the trench was not shaped to fit the contour of the pipe; hence, the pipe had essentially line support along the bottom (Figure 4a). Second, the initial sidefill was placed in a 1-m (3-ft) layer to the springline of the pipe (Figures 4b and 4e), and only the surface of this layer was compacted by small manually operated vibratory tampers. Subsequently, the granular material was placed in approximately 30-cm (1-ft) layers to a height of 1.2 m (4 ft) above the crown of the pipe and compacted with these tampers (Figure 4f). Third, as the sidefill reached the top of the pipe, the groundwater infiltrating the trench virtually saturated the granular material, and several conditions of liquefaction were experienced when attempts were made to compact the sidefill with the tampers. However, as the fill progressed above the pipe, this condition was not encountered with as much severity. Fourth, the backfill from 1.2 to 7.6 m (4 to 25 ft) above the pipe consisted of random mixtures of the two excavated soils, making it virtually impossible to determine with any degree of reliability the point-to-point variations in the mechanical properties of this backfill. This material was compacted with a sheepsfoot roller (Figure 4h), but no specific standards were required or achieved. And fifth, very soon after installation, the groundwater saturated the granular material that enveloped the pipe, and some minor leaks in the pipe system developed. However, these leaks were sealed so that seepage into the pipe was maintained at tolerable levels, and no significantly adverse effects resulted.

**Figure 1. Location of field site.**

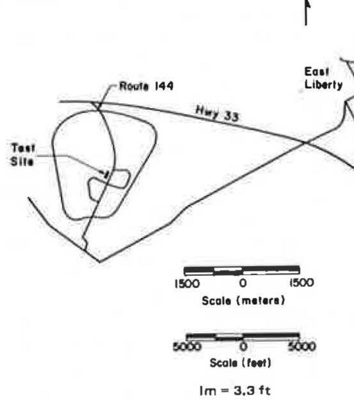


**Figure 2. Longitudinal and cross sections of field installation.**

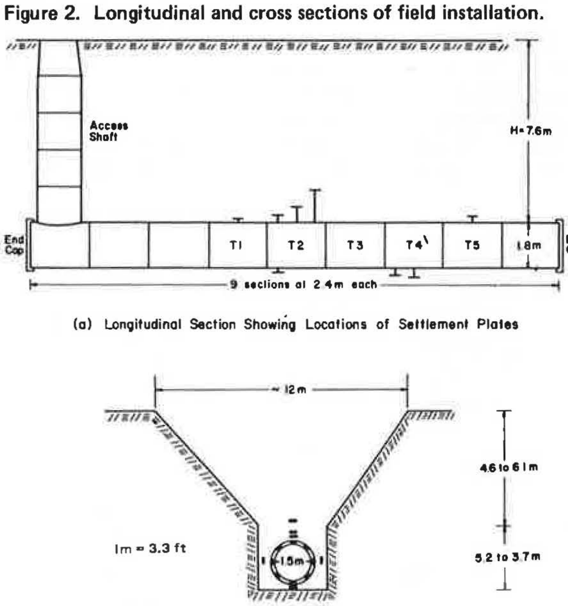


(a) Longitudinal Section Showing Locations of Settlement Plates

(b) Cross Section Showing Locations of Stress Cells

## Stress Distributions

Ten 15-cm (6-in) diameter total stress cells were installed in the wall of the principal pipe (T3, Figure 2); single cells were placed every 45° [alternately in two planes spaced at ±75 cm (30 in) from the midplane] around the pipe with two cells at the top. These cells were placed in recesses made when the pipe was cast, and the surfaces of all cells were flush with the surface of the pipe. In addition, five 25-cm (10-in) diameter total stress cells were placed at discrete points in the soil surrounding the pipe [within 75 cm (2.5 ft) of the pipe]. Three cells were located above the pipe, one below, and one at the springline. The particular locations of these cells relative to the pipe are depicted in the cross-sectional view in Figure 2b. However, the cells were distributed in different transverse planes to avoid interaction among cells. The construction of these cells and an evaluation of their reliability have been reported by Krizek and others (2).

Stress and temperature measurements were obtained from a digital read-out voltmeter and converted to units of gauge pressure. Normal stress distributions around the pipe under various fill heights are shown in Figure 5. Those distributions were drawn by fitting curves to the symmetrized data, which were measured every 45°. The narrowness of the peak at the invert can be explained as an attempt to satisfy vertical equilibrium of normal stresses; furthermore, the fact that the pipe was laid on a flat bed provided for pipe contact with the compacted bedding over an approximately 10° or less arc. However, the following situation regarding vertical equilibrium of normal stresses on the pipe must be

**Figure 3. Log of soil boring at field site.**

| Depth (m) | Standard Penetration Value N | Description | Physical Characteristics: Gravel (%) | Coarse Sand (%) | Fine Sand (%) | Silt (%) | Clay (%) | Liquid Limit (%) | Plasticity Index (%) | Water Content (%) | Class |
|---|---|---|---|---|---|---|---|---|---|---|---|
| 1.5 | 10/7 | Brown Stone Fragments with Sand | - | - | - | - | - | - | - | 13 | - |
| 3.0 | 6/6 | Gray Stone Fragments with Sand | - | - | - | - | - | - | - | 3 | - |
| 4.6 | 6/7 | Gray Sandy Clayey Silt with Stone Fragments | 30 | 9 | 14 | 29 | 18 | 21 | 9 | 12 | A-4a |
| 6.1 | 3/5 | Gray Sandy Clayey Silt | 13 | 9 | 16 | 38 | 24 | 20 | 8 | 12 | A-4a |
| 7.6 | 8/8 | Gray Sandy Clayey Silt | 14 | 9 | 15 | 36 | 26 | 20 | 8 | 12 | A-4a |
| 9.1 | 6/20 | Gray Sandy Clayey Silt with Stone Fragments | 20 | 10 | 15 | 35 | 20 | 20 | 8 | 13 | A-4a |
| | 18/24 | Gray Gravel with Sand | 49 | 24 | 13 | | 14 | NP | NP | 14 | A-1b |
| 10.7 | 16/20 | Gray Stone Fragments with Sand and Silt | 57 | 8 | 9 | 16 | 10 | 21 | 8 | 8 | A-2-4 |
| 12.2 | 10/16 | Gray Sandy Clayey Silt with Stone Fragments | 31 | 12 | 13 | 27 | 17 | 20 | 8 | 10 | A-4a |

1m=3.3ft

**Figure 4. Construction photographs of the test installation.**

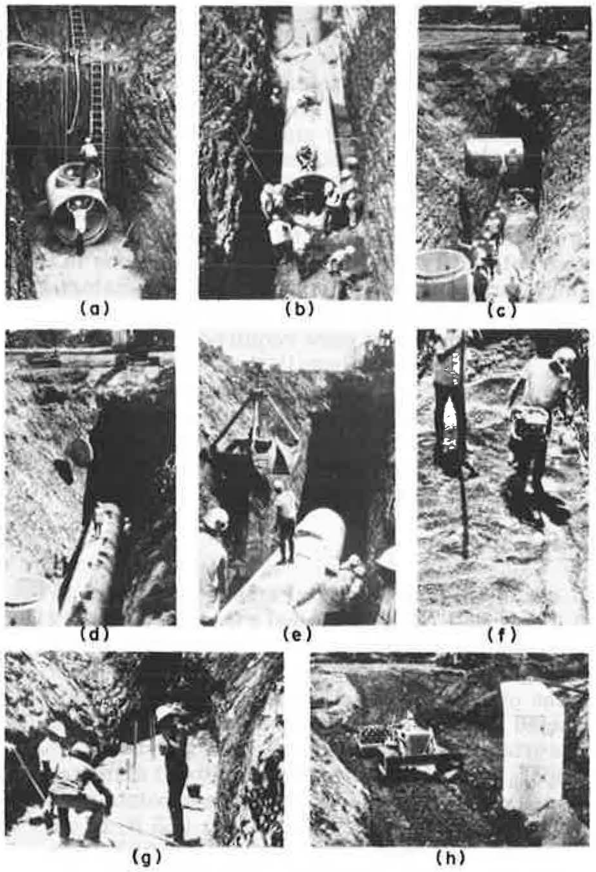


appreciated. The total stress cells measured only normal stresses, and no experimental data were obtained on shear stresses along the soil-pipe interface. Since shear stresses would, in general, not be zero, it follows that the complete stress distribution at the soil-pipe interface has not been obtained, although the satisfaction of equilibrium for an incomplete stress system is not actually necessary. Readings from symmetrically placed cells are reasonably similar, but the resulting stress distributions shown in Figure 5 are quite different from those suggested in the classical Marston-Spangler approach (Figure 6). In assessing the normal stress distribution depicted in Figure 6a, it is important to recall that the support at the bottom of the pipe has been assumed to be very narrow. This is a very substantial assumption and undoubtedly explains much of the difference between the Marston-Spangler analysis and the smoothed experimental curve. In general, the effect of time (stress measurements were taken for approximately 3 years) on the stresses at the soil-pipe interface caused increases of about 10 percent in some cells and no increases in others, with no apparent pattern.

Except for cell S11 at the crown of the pipe, all of the cells apparently functioned properly, although there is some discrepancy in the readings of replicate cells. The fact that cell S11 manifested virtually no increase in stress with an increase in fill height can probably be explained by improper performance of the cell itself (or the presence of an extremely soft spot in the immediate vicinity of the cell). The data from cell S18 have been used to develop the experimental stress distributions at the soil-pipe interface. The pairs of cells symmetrically placed on opposite sides of the pipe at the upper and lower quadrant points gave somewhat different readings, although they all followed consistent trends with increasing fill height. However, the measured differences be-

**Figure 5. Normal stress distributions around pipe in field installation.**

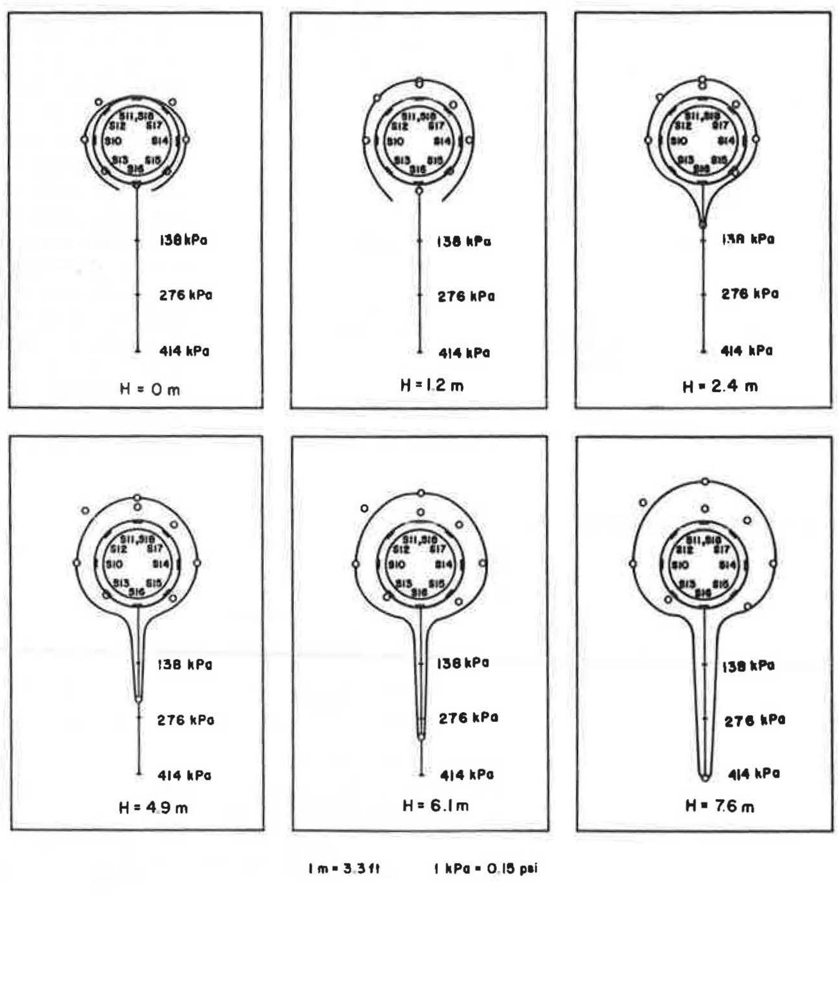


1 m = 3.3 ft    1 kPa = 0.15 psi

tween the readings on the two sides are not great and were probably caused by actual variations in the stresses from local nonhomogeneities in the soil. The cells located on opposite sides of the pipe at the springline gave excellent agreement. The three cells in the soil 15, 30, and 75 cm (6, 12, and 30 in) directly above the pipe yielded stresses that were mutually consistent [readings from the two cells closest to the pipe were essentially similar and slightly higher than that from the cell 75 cm (30 in) above the pipe], but about double the stress from cell S18 in the crown of the pipe. No obvious explanation can be advanced for this phenomenon. The cell 15 cm (6 in) directly below the pipe gave stresses that are somewhat higher (about 30 percent at greater fill heights) than those given by cell S16 embedded in the bottom of the pipe. This situation, as well as the fact that cell S16 yielded disproportionately low readings for low fill heights, suggests that the cell is resting on a low or a soft spot in the bedding. The horizontal stresses measured by the cell embedded in the soil at the springline 23 cm (9 in) from the pipe wall were about two-thirds of the interface stresses measured at the springline, which is entirely consistent with expectations.

Figure 6. Experimental and theoretical normal stresses on pipe at 7.6 m (25 ft) of fill height.

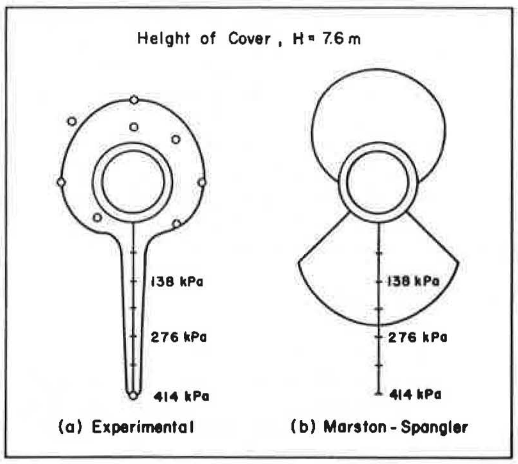


1 m = 3.3 ft    1 kPa = 0.15 psi

Figure 7. Experimental relative displacements between pipe and soil at 7.6 m (25 ft) of fill height.

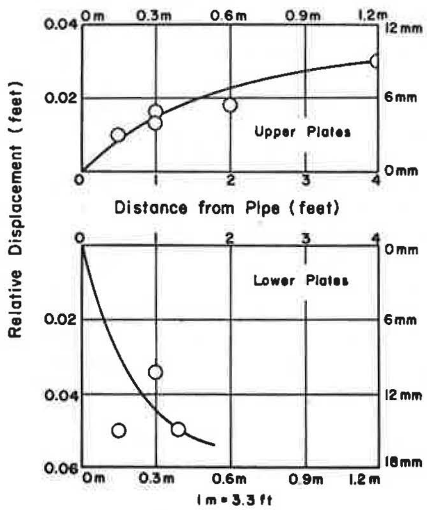


Figure 8. Finite element model of soil-pipe system.

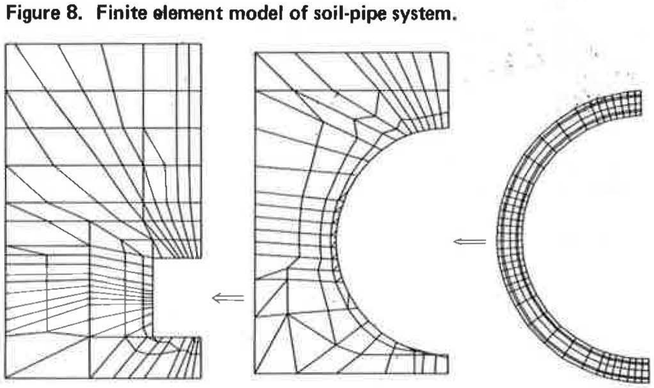

## Soil Displacements

The relative vertical displacements between the pipe wall and various discrete points in the surrounding soil were measured by settlement plates, whose vertical stems passed through sleeves in the crown and invert of the pipe, as illustrated in Figure 2a. Above the pipe, settlement plates were located every 30 cm (12 in) at points 15, 30, 60, and 120 cm (6, 12, 24, and 48 in) from the pipe wall. Settlement plates were also positioned at points 15, 30, and 40 cm (6, 12, and 16 in) below the pipe. The relative displacement between the pipe invert and some fixed benchmark was not measured, so the actual translation of the pipe itself is not known. In general, the relative displacements measured by these plates increased as the height of fill increased and as the distance of the plate from the pipe wall increased. The plots of relative displacement versus distance from the pipe wall are given in Figure 7, and the strain at any point in the soil may be visualized as the slope of the resulting curve at that point. Figure 7 shows that the strains in the soil attenuate rapidly with distance from the pipe wall. This attenuation has been suggested by virtually all continuum models of soil-pipe interaction, but there has been little substantiating experimental evidence.

## COMPATIBILITY OF EXPERIMENTAL MEASUREMENTS

Some appreciation of the reliability of the foregoing experimental measurements can be obtained by examining the mutual compatibility of the data and their consistency with physical evidence. Perhaps the most obvious feature is the high stress intensity measured at the bottom of the pipe. As mentioned previously, this is a direct consequence of the flat bedding employed. Because of the difficulty of compacting the backfill under the haunches of the pipe, relatively low interface stresses would be expected to develop in this area, which was indeed the situation observed. The horizontal stresses developed at the springline indicate that the soil provides considerable lateral support to the pipe, which is consistent with judgment and the measured horizontal diameter changes. The measured interface stresses at the bottom of the pipe are about four times those measured at the top. Considerably greater strains would therefore be expected in the soil below the pipe. The strain in the soil at the soil-pipe interface may be approximated by taking the initial slope of the relative displacement-distance plots shown in Figure 7. Thus it is seen that the strain in the soil below the pipe is about five times that above the pipe. Since the same soil was used above and below the pipe, these comparative values lend considerable support to the argument that the data are mutually compatible. A simple ratio of vertical stress to vertical strain at these points gives a value of 4000 or 5000 kPa (600 or 700 lbf/in$^2$), but it should be cautioned that such a value is useful primarily to identify a reasonable order of magnitude, because the actual stress and strain conditions in the lateral direction are not known. The situation probably cannot be modeled realistically by a uniaxial strain test. Despite some of these discrepancies in the data, the above comparisons and explanations indicate that most of the data reported here are probably within reasonable limits of reliability and accuracy.

## STRESS-STRAIN BEHAVIOR OF SOILS

Piece-wise linear values for the modulus of elasticity and Poisson's ratio were determined from a series of uniaxial strain tests and triaxial compression tests on the granular backfill material used for this installation. Since density is known to exert significant influence on the stress-strain behavior of soils, specimens were tested at three densities: the maximum dry density determined from the standard Proctor compaction test, a density 10 percent above this value, and a density 10 percent below this value. The uniaxial strain tests, which constituted the basis for modulus value determinations in this work, were performed on disc-shaped specimens [about 6.3 cm (0.16 in) in diameter and 2.5 cm (0.06 in) thick] in accordance with the standard loading schedule for consolidation tests. All specimens were saturated prior to testing and allowed to drain freely during testing in order to approximate more closely the field conditions that prevailed at the site. The triaxial compression tests, which provided the basis for determining the value of Poisson's ratio, were conducted by subjecting cylindrical specimens [about 6.3 cm (0.16 in) in diameter and 12.5 cm (0.32 in) long] at approximately optimum water content (as determined from the standard Proctor compaction test) to a constant confining pressure and by increasing the axial load incrementally. Radial displacements were measured directly by means of electronic distance-measuring probes.

Constrained moduli (M) determined from the uniaxial tests were converted to the more conventional modulus of elasticity (E) by using 0.3 for Poisson's ratio ($\nu$) in the relationship $E/M = (1 + \nu)(1 - 2\nu)/(1 - \nu)$. The uniaxial strain test was considered to be more representative of actual field conditions because the stress path in a uniaxial strain test (where the major and minor principal stresses increase proportionately) better approximates that followed by a soil element in the field installation than does the stress path in a triaxial test (in which the major principal stress increases while the minor principal stress is maintained constant, thereby causing unrealistic shear stresses that do not occur in the field). Because of the different stress paths and the resulting shear stresses, the modulus determined from a uniaxial strain test increases with an increase in the mean stress, whereas the opposite is true for the triaxial test. For the range of dry densities tested, initial tangent moduli of approximately 14 000, 7000, and 3500 kPa (2000, 1000, and 500 lbf/in$^2$) were obtained for specimens with the greatest, intermediate, and lowest density respectively. This compares favorably with the experimentally measured 4000 or 5000 kPa (600 or 700 lbf/in$^2$) determined simply by taking the ratio of measured vertical stresses and strains above or below the pipe.

Although the stress-strain properties of the granular backfill were studied rather extensively, the same thoroughness was not applied to the other soils comprising the installation. Two uniaxial strain tests were conducted on specimens trimmed from a block of undisturbed soil taken from the sidewall of the trench at approximately the springline of the pipe, and the results from these tests suggest the use of a constant modulus value of 5600 kPa (800 lbf/in$^2$) for this material. During the process of excavating and backfilling the trench with the natural soils, the materials from the upper and lower layers were mixed in an undetermined manner, and this situation, together with the assortment of rather large stone fragments in the soil and the fact that no specific compaction criteria were enforced, made a realistic determination of any modulus for this material virtually impossible. Hence, modulus values were selected on the basis of previous experience and ranged from about 2800 kPa (400 lbf/in$^2$) under low heights of fill to over 1200 kPa (8400 lbf/in$^2$) for high fill heights. Although no field or laboratory tests were performed on the undisturbed soils beneath the bedding of the pipe, its observed stiffness when the trench was open suggested the use of a high modulus, and a value of 52 000 kPa (7500 lbf/in$^2$) was selected.

## ANALYTICAL COMPARISONS

Certain experimental data were compared with the results calculated from a mathematical model of the soil-pipe system. For this purpose, various supplementary mechanisms were incorporated into the general plane strain (justified on the basis of experimentally measured longitudinal strains in the pipe wall), finite element program (the elements of which are illustrated in Figure 8) developed by Wenzel (4). The program utilizes an empirical cracking mechanism and the mechanical properties of concrete and reinforcing steel to model the pipe (3). The pipe model consists of 320 quadrilateral elements; eight elements (including two overlay elements) are used to model a cross section of the pipe wall. The ability of the mathematical model to duplicate the response of concrete pipe was verified by means of an extensive series of more than 50 controlled load tests on pipes of different diameter, wall thickness, and reinforcement. The validated pipe model was then incorporated into a model of the soil-pipe system by the addition of 257 quadrilateral or triangular soil elements. For the trench installation described here, 97 elements form the in situ soil material, and the rest of the soil elements are added incrementally to simulate the backfill material. Idealized boundary conditions (complete fixity at the vertical and lower horizontal boundaries and complete freedom at the upper horizontal boundary) are assumed at the external boundaries (about one pipe diameter below the pipe and three diameters to each side of the pipe), and a no-slip condition is assumed to exist at the soil-pipe interface.

Since the granular backfill in the vicinity of the pipe was subjected to different degrees of compaction (for instance, the material in the haunch region was dumped in place with virtually no compaction, while the material above and below the pipe and at its springline was compacted rather well) and since the mechanical behavior of this soil is density-dependent (1), the properties assigned to each soil element of the mathematical model were selected to reflect the estimated initial density of that element. As the state of stress in a given element changed with an increase in the height of cover, the modulus of that element varied incrementally. In this way the nonlinear behavior of the soil and its effect on the pipe response were handled in the soil-pipe interaction model.

Typical comparisons between the experimentally

Figure 9. Comparison between experimental and theoretical results.

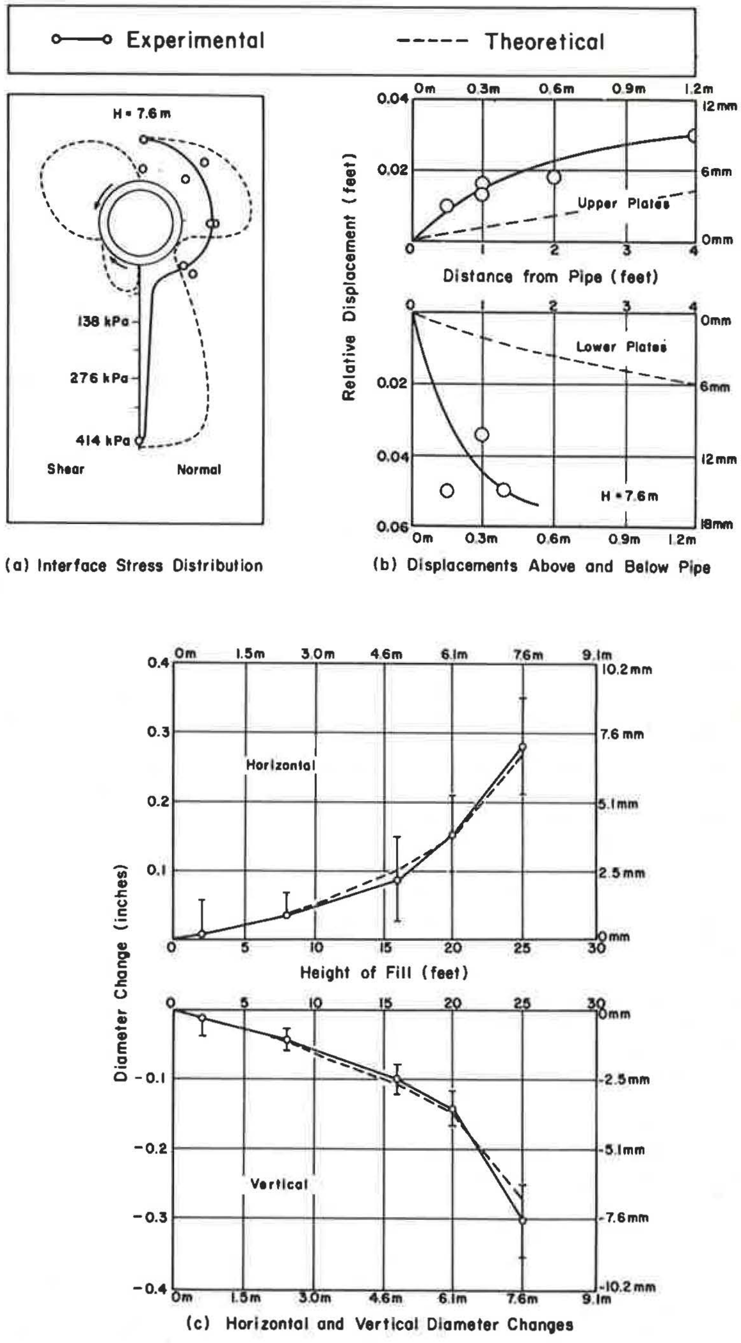


measured data and the results calculated from the mathematical model are given in Figure 9. Of significant importance in Figure 9a is the distribution of shear stresses along the soil-pipe interface. An integration of the vertical components of the computed shear stresses (based on a no-slip condition at the soil-pipe interface) shows that the net downward vertical shear force for the conditions described is essentially equal to the mass of the 1.8-m (6-ft) wide, 7.6-m (25-ft) deep mass of soil above the pipe, and this indicates that interface shear stresses cannot be neglected when establishing the vertical equilibrium of the pipe. Also, the condition of slip at the soil-pipe interface clearly plays a major role in determining the distribution of stresses acting on the pipe and consequently on its associated structural response. Furthermore, the shear stress distribution around the pipe serves to explain to a large degree the apparent concentration of normal stress at the bottom of the pipe. As mentioned previously, shear stresses were not taken into account when best-fit curves were passed through the experimental points shown in Figure 5. The experimental distributions of normal stresses were established on the basis of vertical equilibrium of normal stresses only, thus leading to the sharp peaks illustrated in Figures 5 and 9a. However, since a considerable upward vertical force is necessary to balance the downward force caused by the shear stresses, the normal stresses along the bottom of the pipe must act over a much wider area than that suggested by vertical equilibrium of normal stresses only. Although there are no direct normal stress measurements to document the extent of this area (interface stresses were only measured at 45° intervals), the mathematical model does indicate that high normal stresses act over approximately the bottom 30° to 40° of the pipe, and the predicted intensity of the normal stress at the one point (bottom stress cell) where a measurement was obtained is in reasonable agreement with the measured value. The mathematical model indicates that lateral support by the soil in the haunch region is very low, as would be expected, but the lateral support at the springline of the pipe is substantial, predicted values being somewhat larger than measured values. The theoretical curves for both normal and shear stresses have been smoothed to even out the small discrete jumps between elements with differing mechanical properties. Except for very low heights of cover, the stress cells in the soil both above and below the pipe gave higher readings than the corresponding cells at the soil-pipe interface. Below the pipe the cell at the soil-pipe interface indicated about 420 kPa (60 $lbf/in^2$), and the cell in the soil gave a reading of 550 kPa (80 $lbf/in^2$) for a fill height of 7.6 m (25 ft). This observation might be explained by supposing that the interface cell rested on a soft or low spot in the bedding, although this is not known for certain. For the cells at 0, 15, 30, and 75 cm (0, 6, 12, and 30 in) above the pipe, the normal stresses under 7.6 m (25 ft) of fill were 97, 186, 242, and 152 kPa (14, 27, 35, and 22 $lb/in^2$) respectively, and the explanation is not so apparent. Although the mathematical model also indicates a slight increase in stress with distance above the pipe up to a few feet or a meter, this difference is not nearly as large as the measured difference. One explanation for the higher measured stresses is the possibility that the cells embedded in the soil might actually be "hard spots" that attract disproportionately high stresses, but this is not supported by the experience with these cells in other field locations and in laboratory calibration (2).

The calculated relative displacements between the pipe wall and discrete points in the adjacent soil, as shown in Figure 9b for 7.6 m (25 ft) of cover, are considerably lower than the measured values both above and below the pipe. Although no specific reason can be given for this discrepancy, the reliability of the field data is supported by the facts that (a) the ratio of the measured relative displacements below the pipe to those above the pipe is reasonably consistent with the corresponding ratio of the measured stresses at those two locations and (b) the approximate modulus values determined by simply taking the ratio of the measured vertical stresses to the measured vertical strains at these locations are in good agreement with moduli measured in laboratory stress-strain tests on specimens with comparable dry densities. These comparisons of stresses and displacements at discrete points constitute severe criteria by which to evaluate the ability of the mathematical model to predict experimental results, because they represent point values in a very heterogeneous system. Diameter changes, on the other hand, represent a more spatially integrated behavior. The horizontal and vertical diameter changes were measured at the center of each of the five test sections by a specially constructed portable extensometer. This instrument, which was fitted between stainless steel spheres epoxied to the inside pipe wall, was adjusted to have constant compressive force for all readings. Shown in Figure 9c are the mean and range of the five readings for each fill height. As this figure shows, the agreement between the measured and modeled changes in the vertical and horizontal diameters of the pipe is excellent.

## CONCLUSIONS

Based on the limitations of the results reported here, certain conclusions can be drawn. First, with few exceptions the measured stresses and displacements at discrete points in the experimental installation are mutually consistent and compatible with judgment and previous experience. Second, although the stresses and displacements calculated at discrete points by a plane strain, finite element model are at variance with the corresponding experimental measurements, the excellent agreement between experimentally measured and theoretically calculated horizontal and vertical diameter changes of the pipe indicates that the ability of the mathematical model to predict the overall experimental behavior is very good. Third, both the experimental and theoretical distributions of interface stresses around the pipe are different from those suggested in the Marston-Spangler approach. Fourth, the soil at the springline of the pipe is capable of giving considerable lateral support to the pipe and, except for the higher stress levels at the bottom of the pipe and the lower stresses in the haunch region, the measured interface stresses around the pipe were nearly hydrostatic.

## ACKNOWLEDGMENTS

This work was performed as part of an extensive research effort supported by the American Concrete Pipe Association to investigate the soil-structure interaction of buried concrete pipe. The soil tests and much of the original data reduction were performed by M. Hassan Farzin.

## REFERENCES

1. R. J. Krizek and R. B. Corotis. Synthesis of Soil Moduli Determined From Different Types of Laboratory and Field Tests. Proc., Specialty Conference on in Situ Measurement of Soil Properties, ASCE, June 1975, pp. 225-240.
2. R. J. Krizek, M. H. Farzin, A. E. Z. Wissa, and R. T. Martin. Evaluation of Stress Cell Performance. Journal of Geotechnical Engineering Division, ASCE, Vol. 100, No. GT12, 1974, pp. 1275-1295.
3. R. A. Parmelee. Investigation of Soil-Structure Interaction of Buried Concrete Pipe. HRB, Highway Research Record 443, 1973, pp. 32-39.
4. T. H. Wenzel. The Design and Response of Circular Concrete Pipe. Department of Civil Engineering, Northwestern Univ., Evanston, Ill., PhD dissertation, 1975.

*Publication of this paper sponsored by Soil Mechanics Section.*

**Mr. Wenzel was a research assistant in the Department of Civil Engineering, Northwestern University, when this research was done.*